# Morphology, structure, optical property and photoelectrochemical property of $TiO_2$ nanoflower films synthesised via liquid phase deposition technique

*M.Y.A. Rahman[1], A.A. Umar[1], L. Roza[1,2], M.M. Salleh[1]*

[1]*Institute of Microengineering and Nanoelectronics (IMEN), Universiti Kebangsaan Malaysia, Bangi 43600, Selangor, Malaysia*
[2]*College of Foundation and General Studies, Universiti Tenaga Nasional, Kajang 43009, Selangor, Malaysia*
*E-mail: mohd.yusri@ukm.my*

Published in Micro & Nano Letters; Received on 14th January 2014; Revised on 16th February 2014; Accepted on 12th March 2014

This reported study was concerned with the synthesis of $TiO_2$ nanoflowers as a photovoltaic material of the photoelectrochemical cell (PEC) via the phase liquid deposition technique. It highlighted the effect of the growth time on the morphology of $TiO_2$ samples. Three growth times were chosen, namely 2, 4 and 6 h. The morphology was examined by scanning electron microscopy (SEM). The nanoflowers' morphology of the $TiO_2$ sample grown for 4 h was then chosen to be characterised by cross-sectional SEM, X-ray diffraction, ultraviolet–visible and photoelectrochemical measurement. The sample was crystalline with anatase phase. The sample showed the strongest absorption at 330 nm. The $TiO_2$ nanoflowers PEC demonstrated the $J_{sc}$ and $V_{oc}$ of 0.046 $mAcm^{-2}$ and 0.26 V, respectively.

**1. Introduction:** Various synthesis and deposition techniques have been applied in preparing $TiO_2$ nanostructures, such as sputtering, chemical vapour deposition, spray pyrolysis [1], anodic oxidation [2, 3], hydrothermal synthesis [4], template synthesis, sol–gel fabrication [5] and many more. Each technique produces unique morphologies of the $TiO_2$ nanostructures, such as nanowire [6], nanofibre [7], nanorods and nanotube arrays [2] to overcome the shape limitation of $TiO_2$ nanoparticle morphology. The ability to control the surface morphology and thickness of the $TiO_2$ nanoparticle film on the transparent conducting substrate is important in all applications that are based on the cells related to the compact and dense surface of $TiO_2$ nanoparticles.

Liquid phase deposition (LPD) was chosen for synthesising $TiO_2$ nanoparticles in this reported study, since this technique is simple, quick and cheap. Deki *et al.* [8] first reported the synthesis of $TiO_2$ via this technique. His research group has successfully synthesised $TiO_2$ nanostructures by simply mixing the $(NH_4)_2TiF_6$ and $H_3BO_3$ solutions. The morphology of $TiO_2$ nanostructures could be tuned by modifying the synthesis parameters such as deposition time, growth temperature and precursor solution.

In this study, the morphology of $TiO_2$ nanostructures was modified by adjusting the growth time of the LPD technique, namely 2, 4 and 6 h. The new idea of this Letter was the use of $TiO_2$ nanoflowers that were prepared via the above technique in a photoelectrochemical cell (PEC). The objective of this study was to investigate the effect of deposition time on the morphology of the $TiO_2$ sample. The $TiO_2$ sample with the deposition time of 4 h that resulted in $TiO_2$ nanoflowers with the most compact and dense morphology was chosen for cross-sectional scanning electron microscopy (SEM) characterisation to determine the structural, optical and photoelectrochemical properties.

## 2. Experimental

2.1. Materials: The raw materials for the preparation of the $TiO_2$ nanostructure included ITO substrate purchased from Vin Karola Instruments, USA. Ammonium hexafluorotitanate (metal-fluoro complex) and boric acid that serve as fluoride scavengers were purchased from Sigma-Aldrich, and Wako Chemicals, USA, respectively. An electrolyte that contains 0.5 M LiI/0.05 M $I_2$/0.5 M *tert*-butylpyridine (TBP) in acetonitrile was purchased from Fluka and Sigma-Aldrich. Platinum powder needed for the preparation of the counter electrode of the PEC was purchased from Solaronix.

2.2. Synthesis of $TiO_2$ nanostructures: ITO substrates were cut into a desired size and cleaned with distilled water using cotton buds to remove any dust. The substrates were then immersed in acetone in an ultrasonic bath for 15 min to remove particles and organic contaminations. The substrates were then rinsed with deionised water. The substrates were then immersed for another 15 min in 2-propanol in an ultrasonic bath, and then rinsed immediately with 2-propanol to remove the metal contaminant and an organic binder. The substrates were then dried with purified nitrogen gas to ensure the substrates were cleaned and dried thoroughly. After the cleaning treatment, the substrates were used immediately for the deposition process. $TiO_2$ nanostructures were grown and deposited directly on the substrate via the LPD process. The cleaned substrate was placed vertically in a freshly prepared solution containing 5 ml $(NH_4)_2TiF_6$ with 0.1 M concentration and 5 ml $H_3BO_3$ with 0.2 M concentration. The substrate was then immersed in the solution at 50°C for 4 h and then taken out of the solution. The sample was cleaned with acetone to remove the residual solution on the glass side. The coated substrate was dried with a nitrogen flow at room temperature. Finally, the sample was annealed in a furnace at 400°C for 1 h to remove any organic binder. These procedures were repeated for the growth times of 2 and 6 h, respectively.

Field-emission SEM (FESEM) model Zeiss Supra 55VP FESEM was employed to observe the morphology in terms of the shape and grain size of the $TiO_2$ nanostructures. The magnification of 10 000× was chosen to investigate the morphology of the samples. FESEM was also employed to measure the thickness of the samples by the cross-sectional view. The structure and phase structure of the $TiO_2$ samples were examined by X-ray diffraction (XRD) model Bruker D8 Advance measurements using Cu $K_\alpha$ radiation generated at energy of 40 kV and current of 40 mA, which emits a wavelength of 15.4 nm. The XRD patterns of the samples were recorded in the range of a 10° to 60° diffraction angle. An optical spectrophotometer UV–vis Lambda 900 Perkin Elmer was employed to study the optical absorption of the $TiO_2$ sample. The absorbance of the films was measured in the wavelength ranging from 300 to 900 nm.

2.3. Fabrication and performance study of PEC: The preparation of $TiO_2$ nanoflowers as a photovoltaic material has been described in the Experimental section. Platinum film as a counter electrode was prepared by sputtering platinum pellets on the ITO substrate. An

electrolyte containing 0.5 M LiI/0.05 M $I_2$/0.5 M TBP in acetonitrile was used as a redox couple. The electrolyte was sandwiched between the $TiO_2$ nanoflowers film and the counter electrode. The cell was clamped to optimise the interfacial contact between the layers making up the cell. The performance study of the cell was carried out by observing the current–voltage in the dark and under illumination using an AM 1.5 simulated light with an intensity of 100 $mWcm^{-2}$. The illuminated area of the cell was 0.24 $cm^2$. The current–voltage curves in the dark and under illumination were recorded by a Keithley high-voltage source model 237 interfaced with a personal computer.

**3. Results and discussion:** Figs. 1*a–c* show the FESEM images of the $TiO_2$ nanostructure for deposition times of 2, 4 and 6 h, respectively. Flower-like $TiO_2$ nanostructures were successfully formed onto ITO-coated glass. In Fig. 1*a*, flower-like structures with a diameter in the range of 20 nm were observed, together with big flower-like agglomerated particles with an average diameter of 120 nm. However, the particles only partially covered the substrate and empty spaces remained on the substrate. This means that this growth time was insufficient to completely cover the substrate. The morphology of the $TiO_2$ nanoflowers for the growth time of 4 h was described in terms of a well formed, high density and compact structure. The $TiO_2$ nanostructures were observed to be grown on the large area of the substrate. On the other hand, the morphology appeared to be slightly waved with a flower-like structure. A large number of non-uniform agglomerates were observed on the entire surface of the ITO substrate. The typical morphology of the $TiO_2$ nanostructures shows the mixture of almost spherical and flower-like structures with a high porosity $TiO_2$ structure surface, which can clearly be observed at high magnification, as shown in Fig. 1*b*. As observed from the FESEM micrograph, the $TiO_2$ nanoflowers showed irregular shape and the grain sizes of this sample are not identical, but are slightly larger in diameter than that of the growth time of 2 h. The morphology of the $TiO_2$ nanostructure contained a large amount of closely-packed particles with a porous structure as shown in low magnification micrograph (inset of Fig. 1*b*).

In contrast, the morphology of the sample for the growth time 6 h was found to show a flower-like morphology $TiO_2$ nanostructure with a sharper tip and agglomerate formed on the surface of $TiO_2$ nanostructure. Additionally, compact nanoparticles $TiO_2$ substrate coverage and cracks were observed. The increase in surface tension of the $TiO_2$ nanoflowers could be linked to increase in the growth time [9–11]. Flower-like $TiO_2$ nanostructures were mainly observed for the growth time 2 h until 6 h, but differ in density and grain size. The particle size of $TiO_2$ nanoflowers films was in 10–25 nm range. The grain size of this sample was smaller than that reported by Gutierrez-Tauste *et al.* [12] and Liao *et al.* [13] and higher than $TiO_2$ samples prepared by Mathew *et al.* [14]. In conclusion, the growth time of 4 h demonstrated the best morphology, as shown in Fig. 1*b*; the $TiO_2$ nanoflowers film was found to cover the entire substrate surface, which produced a high porous structure. The morphology and density of $TiO_2$ nanostructure depend on deposition time as reported in [9]. The high-density $TiO_2$ nanostructure synchronised with a compact structure without any cracks and cavities enhanced the contact between the $TiO_2$ nanostructure and the ITO to provide more electron pathways for photo-regenerated electrons [15]. This condition is demanded in PEC application for facilitating a more efficient redox reaction.

Fig. 2 shows the cross-sectional FESEM image of the $TiO_2$ sample deposited for 4 h at 50°C on ITO-coated glass substrate. The cross-sectional view shows that the thickness of the $TiO_2$ nanoflowers film was about 350 nm. The cross-sectional image also confirmed that the $TiO_2$ nanoflowers with the growth time of 4 h produced a high density and porous structure surface. The porous structure of the $TiO_2$ sample can absorb more ions from the electrolyte.

Fig. 3 shows the XRD pattern of the $TiO_2$ sample deposited for 4 h. The sample exhibited the formation of a single phase with a body-centred tetragonal. All the peaks were indexed with their index Miller (*hkl*). After annealing at 400°C for 1 h, the sample was converted into anatase phase. The structure of the sample was crystalline with a high degree of crystallinity indicated by sharp and broad peaks diffraction with low noise observed. The growth orientation was towards the [101] and [004] direction crystalline phase with preferred anisotropic growth along the *c*-axis of the anatase phase. Meanwhile, the diffraction peak of the anatase phase at the [101] direction indicated the strongest intensity and broadest peak. On the other hand, the [004] peak was relatively lower in intensity than the [101] peak. The intensity ratio of [101] to [004] was 2:1, indicating a high degree crystallinity of the sample and dominant growth at the [101] direction plane. The

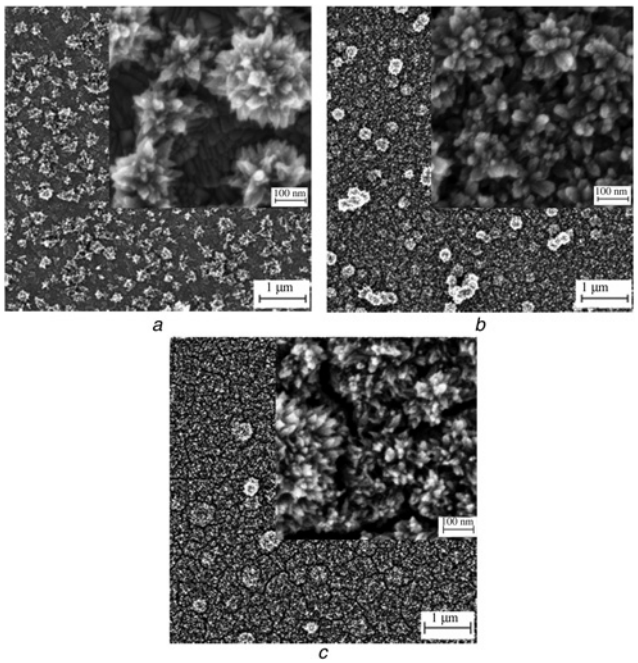


**Figure 1** *FESEM images of $TiO_2$ nanoflowers film at different deposition times*
*a* 2 h
*b* 4 h
*c* 6 h

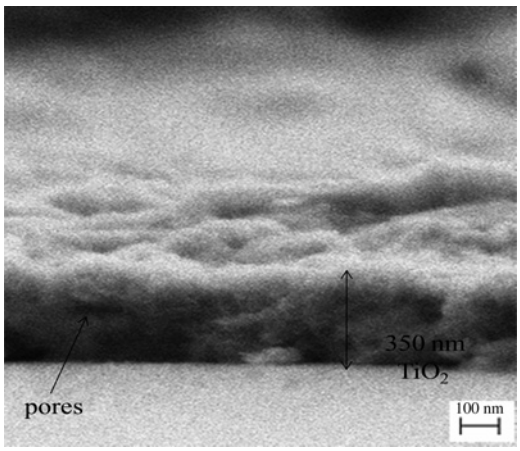


**Figure 2** *Cross-sectional FESEM image of $TiO_2$ nanoflowers deposited for 4 h*




doi: 10.1049/mnl.2014.0017

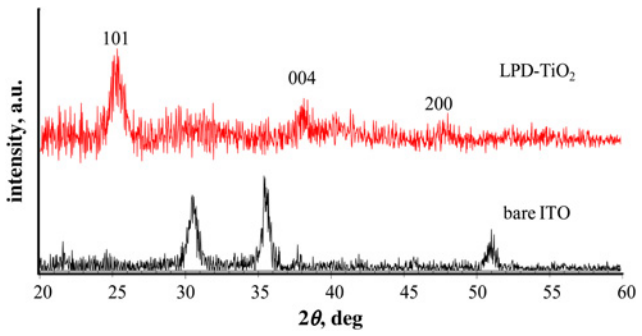


**Figure 3** *Typical XRD pattern of $TiO_2$ nanoflowers deposited for 4 h*

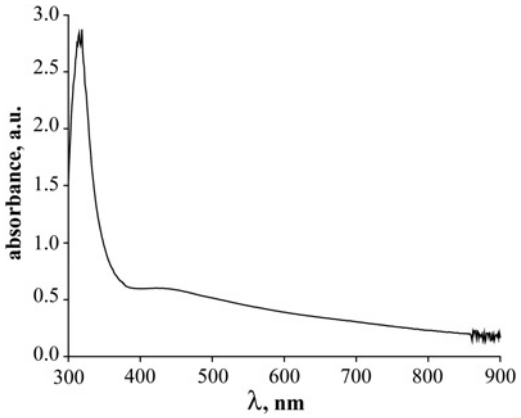


**Figure 4** *UV–vis spectrum of $TiO_2$ nanoflowers deposited for 4 h*

result agreed well with that reported in [16]. The crystallite size of the sample was found to be 25 nm.

Fig. 4 shows the UV–vis absorption spectrum of the sample deposited for 4 h. The curve indicates the appearance of the absorption spectrum in the wavelength ranges from visible light to near infrared. It is observed from the Figure that the sample shows strong absorption at the wavelength less than 370 nm, similar to the $TiO_2$ sample that absorbed UV light at the wavelength less than 350 nm

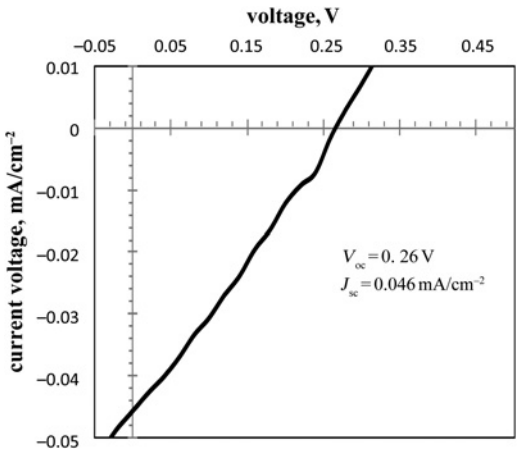


**Figure 5** *J–V curve of the PEC fabricated with $TiO_2$ nanoflowers under light illumination*

reported by Wang *et al.* [17]. The spectrum of the sample deposited for 4 h displays a prominent absorption near the blue region (350–400 nm).

Fig. 5 shows the current density–voltage curve of the PEC under light illumination. The analysis on the curve indicated that the $J_{sc}$ and $V_{oc}$ of the device were 0.046 mA and 0.26 V, respectively. The fill factor obtained from the curve was 0.28. The small current generated in the device was due to a large bandgap of $TiO_2$, resulting in a poor response to the light in the visible region, as depicted in Fig. 4. A small amount of light was absorbed by the $TiO_2$ layer, leading to a small number of electron-hole pairs generated in the cell. The $J_{sc}$ and $V_{oc}$ of the cell were larger than those of $TiO_2$ PEC reported by Rahman *et al.* [18], which were 0.95 $\mu Acm^{-2}$ and 180 mV, respectively. The $J_{sc}$ was about 48 times higher than reported in the literature since the ionic conductivity of the liquid electrolyte used in this study was much higher than the solid polymeric electrolyte of PVC-PC-$LiClO_4$ used in the PEC reported in [18]. Higher conductivity resulted in a faster redox reaction at the interface of the electrolyte/$TiO_2$. Electrons were replaced with other electrons more quickly, thus improving the performance of the cell [18].

**4. Conclusion:** $TiO_2$ nanoflowers were successfully synthesised via the LPD technique for various growth times, namely 2, 4 and 6 h. It was found that the sample grown for 4 h possessed the most compact and dense morphology. The sample was crystalline with anatase phase. The sample showed the strongest absorption at 330 nm. The cell utilising the $TiO_2$ sample demonstrated the photovoltaic effect with the $J_{sc}$ and $V_{oc}$ of 0.046 $mAcm^{-2}$ and 0.26 V, respectively.

**5. Acknowledgment:** This Letter was supported by the Ministry of Higher Education of Malaysia under research grant FRGS 011010118.

## 6 References

[1] Tachan Z., Ruhle S., Zaban A.: 'Dye-sensitized solar tubes: A new solar cell design for efficient current collection and improved cell sealing', *Sol. Energy Mater. Solar Cells*, 2010, **94**, pp. 317–322

[2] Paulose M., Shankar K., Varghese O.K., Mor G.K., Grimes C.A.: 'Application of Highly-ordered TiO2 Nanotubes-Arrays in Heterojuction Dye-Sensitized Solar Cell', *J. Phys. D, Appl. Phys.*, 2006, **39**, p. 2498

[3] Xu T., Lin J., Chen X.: 'The Effect of Pre-Pattern on The Morphology and Growht Speed of TiO2 Nanotubes', *Appl. Surf. Sci.*, 2011, **258**, pp. 76–80

[4] Dhas V., Muduli S., Agarkar S., *ET AL.*: 'Enhanced DSSC performance with high surface area thin Anatase TiO2 nanoleaves', *Sol. Energy*, 2011, **85**, pp. 1213–1219

[5] Bak Y.-R., Kim G.-Ok., Hwang M.-J., Cho K.-K., Kim K.-W., Ryu K.-S.: 'Fabrication and Performance of Nanoporous TiO2/SnO2 Electrodes with a Half Hollow Sphere Structure for Dye Sensitized Solar Cells', *J. Sol Gel Sci. Technol.*, 2011, **58**, pp. 518–523

[6] Wei Z., Li R., Huang T., Yu A.: 'Fabrication of morphology controllable rutile TiO2 nanowire arrays by solvothermal route for dye-sensitized solar cells', *Electrochim. Acta*, 2011, **56**, pp. 7696–7702

[7] Kim J.-U., Park S.-H., Choi H.-J., Lee W.-K., Lee J.-K., Kim M.-R.: 'Effect of electrolyte in electrospun poly(vinylidene fluoride-co hexafluoropropylene) nanofibers on dye-sensitized solar cells', *Solar Energy Mater. Solar Cells*, 2009, **93**, pp. 803–807

[8] Deki S., Hnin Y.Y.K., Fujita T., Akamatsu K., Mizuhata M., Kajinami A.: 'Synthesis and microstructure of metal oxide thin films containing metal nanoparticles by liquid phase deposition (LPD) method', *Eur. Phys. J. D*, 2001, **16**, pp. 325–328

[9] Zhang J., Yang C., Chang G., Zhu H., Oyama M.: 'Voltammetric behavior of TiO2 films on graphite electrodes prepared by liquid phase deposition', *Mater. Chem. Phys.*, 2004, **88**, pp. 398–403

[10] Zhang J., Oyama M.: 'Tunable electrochemical properties of liquid phase deposited TiO2 films', *J. Appl. Electrochem.*, 2008, **38**, pp. 1421–1426

[11] Jiang G., Tang H., Zhu L., Zhang J., Lu B.: 'Improving electrochemical properties of liquid phase deposited TiO2 thin films by doping sodium dodecylsulfonate and its application as bioelectrocatalytic

sensor for hydrogen peroxide', *Sens. Actuators B, Chem.*, 2009, **138**, pp. 607–612
[12] Gutierrez-Tauste D., Domenech X., Domingo C., Ayllon J.A.: 'Dopamine/TiO2 hybrid thin films prepared by the liquid phase deposition method', *Thin Solid Films*, 2008, **516**, pp. 3831–3835
[13] Liao C.-H., Shih W.-T., Chen C.-C., Lee Y.-L., Kuo P.-L.: 'Effect of photoelectrode morphology of single-crystalline anatase nanorods on the performance of dye-sensitized solar cells', *Thin Solid Films*, 2011, **519**, pp. 5552–5557
[14] Mathew A., Rao G.M., Munichandraiah N.: 'Effect of TiO2 electrode thickness on photovoltaic properties of dye sensitized solar cell based on randomly oriented Titania nanotubes', *Mater. Chem. Phys.*, 2011, **127**, pp. 95–101
[15] Ito S., Murakami T.N., Comte P., *ET AL.*: 'Fabrication of thin film dye sensitized solar cells with solar to electric power conversion efficiency over 10%', *Thin Solid Films*, 2008, **516**, pp. 4613–4619
[16] Rahman M.Y.A., Umar A.A., Roza L., Salleh M.M.: 'Effect of cetyltrimethyl ammonium bromade surfactant concentration on the physical and photoelectrochemical property of TiO2 nanowire', *Int. J. Electroactive Mater.*, 2013, **1**, pp. 28–35
[17] Wang R., Zhang J., Hu Y.: 'Liquid Phase Deposition of Hemoglobin/SDS/TiO2 Hybrid Film Preserving Photoelectrochemical Activity', *Bioelectrochemistry*, 2011, **81**, pp. 34–38
[18] Rahman M.Y.A., Salleh M.M., Talib I.A., Yahaya M., Ahmad A.: 'Current transport mechanism and photovoltaic properties of photoelectrochemical cell of ITO/TiO2/PVC-LiClO4/graphite', *Curr. Appl. Phys.*, 2007, **7**, pp. 446–449




doi: 10.1049/mnl.2014.0017